HHS Public Access

Author manuscript

J Nucl Med. Author manuscript; available in PMC 2016 February 03.

Published in final edited form as:

J Nucl Med. 2016 February ; 57(2): 186–191. doi:10.2967/jnumed.115.161018.

[^{68}Ga]-DOTATATE PET/CT in the localization of head and neck paragangliomas compared to other functional imaging modalities and CT/MRI

Ingo Janssen, MD[1,8], **David Taieb, MD, PhD**[2], **Nicholas J. Patronas, MD**[3], **Corina M. Millo, MD**[4], **Karen Adams, CRNP, MSc**[1], **Joan Nambuba, BS**[1], **Clara C. Chen, MD**[5], **Peter Herscovitch, MD**[4], **Samira M. Sadowski, MD**[6], **Antonio T. Fojo, MD, PhD**[7], **Inga Buchmann, MD**[8], **Electron Kebebew, MD**[6], and **Karel Pacak, MD, PhD, DSc**[1]

Ingo Janssen: ingo.janssen@nih.gov

[1]Program in Adult and Reproductive Endocrinology, Eunice Kennedy Shriver National Institute of Child Health and Human Development, National Institutes of Health, 10 Center Dr., Bldg. 10, Room 1E-3140, Bethesda, MD, 20892

[2]Department of Nuclear Medicine, La Timone University Hospital, CERIMED, Aix-Marseille University, Marseille, France

[3]Section of Neuroradiology, Radiology and Imaging Sciences, Warren Grant Magnuson Clinical Center, National Institutes of Health, 10 Center Dr., Bldg. 10, Bethesda, MD, 20892

[4]Positron Emission Tomography Department, Warren Grant Magnuson Clinical Center, National Institutes of Health, 10 Center Dr., Bldg. 10, Rooms 1C-401 and 490, Bethesda, MD, 20892

[5]Nuclear Medicine Division, Radiology & Imaging Sciences, Warren Grant Magnuson Clinical Center, National Institutes of Health, 10 Center Dr., Bldg. 10, Room 1C-459, Bethesda, MD, 20892

[6]Endocrine Oncology Branch, National Cancer Institute, 10 Center Dr., Bldg. 10, Bethesda, MD, 20892

[7]Center for Cancer Research, National Cancer Institute, 10 Center Dr., Bldg. 10, Room 12C-103, Bethesda, MD, 20892

[8]Department of Radiology and Nuclear Medicine, Section of Nuclear Medicine, University Hospital Schleswig Holstein, Campus Lübeck, Ratzeburger Allee 160, 23538 Lübeck, Germany

Abstract

Pheochromocytomas/paragangliomas (PHEOs/PGLs) overexpress somatostatin receptors (SSTRs) and recent studies have already shown excellent results in the localization of sympathetic succinate dehydrogenase complex, subunit *B (SDHB)* mutation-related metastatic PHEOs/PGLs using [(^{68}Ga)-DOTA0,Tyr3]Octreotate ([^{68}Ga]-DOTATATE) positron emission tomography/

Corresponding author: Karel Pacak, MD, PhD, DSc, Senior Investigator, Chief, Section on Medical Neuroendocrinology, Professor of Medicine, Eunice Kennedy Shriver NICHD, NIH, Building 10, CRC, Room 1E-3140, 10 Center Drive MSC-1109, Bethesda, MD, 20892, Phone: (301) 402-4594, Fax: (301) 402-4712, karel@mail.nih.gov.

First author: Ingo Janssen, MD, Visiting Fellow, *Eunice Kennedy Shriver* NICHD, NIH, Building 10, CRC, Room 1E-3140, 10 Center Drive MSC-1109, Bethesda, MD, 20892, Phone: (301) 402-4594, Fax: (301) 402-4712

computed tomography (PET/CT). Therefore, the goal of our study was to assess the clinical utility of this functional imaging modality in parasympathetic head and neck paragangliomas (HNPGLs) compared to anatomical imaging with CT/MRI and other functional imaging modalities, including [^{18}F]-fluorohydroyphenylalanine ([^{18}F]-FDOPA) PET/CT, currently the gold standard in the functional imaging of HNPGLs.

Methods—[^{68}Ga]-DOTATATE PET/CT was prospectively performed in 20 patients with HNPGLs. All patients also underwent [^{18}F]-FDOPA PET/CT, [^{18}F]-fluoro-2-deoxy-D-glucose ([^{18}F]-FDG) PET/CT, and CT/MRI, with 18 patients also receiving [^{18}F]-fluorodopamine ([^{18}F]-FDA) PET/CT. [^{18}F]-FDOPA PET/CT and CT/MRI served as the imaging comparators.

Results—Thirty-eight lesions in 20 patients were detected, with [^{18}F]-FDOPA PET/CT identifying 37 of 38 (37/38) and CT/MRI identifying 22 of 38 lesions (22/38, $p<0.01$). All 38 and additional 7 lesions ($p=0.016$) were detected on [^{68}Ga]-DOTATATE PET/CT. Significantly fewer lesions were identified by [^{18}F]-FDG PET/CT (24/38, $p<0.01$) and [^{18}F]-FDA PET/CT (10/34, $p<0.01$).

Conclusion—[^{68}Ga]-DOTATATE PET/CT identified more lesions than the other imaging modalities. Due to the results of the present study, including the increasing availability and use of DOTA-analogs in the therapy of neuroendocrine tumors, we expect that [^{68}Ga]-DOTATATE PET/CT will become the preferred functional imaging modality for HNPGLs in the near future.

Keywords

[^{68}Ga]-DOTATATE; [^{18}F]-FDOPA; head and neck paraganglioma

Introduction

Head and neck paragangliomas (HNPGLs) are neuroendocrine tumors derived from the parasympathetic nervous system (1, 2), representing approximately 0.6% of all head and neck tumors (3). These tumors mainly occur in the carotid body (CB), glomus vagale (GV), glomus jugulare (GJ), or glomus tympanicum (GT) regions. However, PGLs have also been reported in the larynx, nasopharynx, orbit, or sinonasal areas (2). Depending on their localization and multiplicity, up to 38% or even more of HNPGLs in patients with a negative family history are hereditary (4). The majority of hereditary HNPGLs belong to patients with succinate dehydrogenase complex, subunits *B, C*, or *D (SDHB, SDHC, SDHD*, collectively *SDHx)* mutations. More than 50% belong to *SDHD* mutations, but *SDHB* and *SDHC* mutations are seen in about 20%-35% and 15% of patients, respectively (4-6).

CB tumors are most common (60%), followed by PGLs of the GJ (23%), GV (13%), and GT (6%) (7). Although patients with hereditary HNPGLs are at a high risk for metastatic disease (patients with *SDHB* mutations) or prone to developing multiple HNPGLs, especially those with *SDHD* mutations (8), proper diagnosis of these tumors is often challenging since HNPGLs are typically biochemically silent and lack early symptoms (7).

Anatomical and functional imaging studies are important for the proper localization of these tumors, including the detection of any multiplicity and surrounding tissue involvement, all

paramount in the assessment of which treatment options to use. A failure of such precise assessment of these tumors usually leads to catastrophic consequences.

Anatomical imaging techniques such as computed tomography (CT) and magnetic resonance imaging (MRI) are nonspecific but crucial for the initial diagnosis and, particularly, delineation of these tumors. Functional imaging modalities enable whole body imaging and are more specific since they address particular receptors and transporters, which are supposed to be upregulated in HNPGLs (9). [^{18}F]-fluorohydroxyphenylalanine ([^{18}F]-FDOPA) positron emission tomography (PET)/CT is currently the functional imaging modality of choice in HNPGLs according to previous studies (2, 10-12) and the current guidelines (13, 14) in that it provides a higher sensitivity than anatomical imaging with CT and/or MRI and a specificity ≥95% (2, 10-12).

PGLs are known to overexpress somatostatin receptors (SSTR), especially SSTR2 (15), and [^{68}Ga]-DOTA-peptides bind to SSTR expressing tumors much more effectively compared to [^{111}In]-DTPA-octreotide (16), which is still the second recommended functional imaging tool for HNPGLs (13). Furthermore, DOTA-peptides can be labeled with the therapeutic beta-emitters [^{177}Lu] or [^{90}Y] and used for peptide receptor radionuclide therapy (PRRT). Since therapeutic approaches for these patients, especially those with multiple or surgically non-approachable tumors, are still very limited, PRRT and treatment with so-called “cold” synthetic somatostatin analogs (SSA) like octreotide or lanreotide could be important new treatment options, especially since they have already been successfully performed in a few patients with HNPGLs (17-19).

The excellent performance of [^{68}Ga]-DOTA-peptides in (genetically not further evaluated) HNPGLs was already reported (20, 21) as well as their excellent performance in localizing metastatic *SDHB* related PHEOs/PGLs outside the head and neck region (22).

Therefore, our first aim was to: a) evaluate the diagnostic utility of [^{68}Ga]-DOTATATE PET/CT in *SDHB* and/or *SDHD (SDHx)* related and other HNPGLs compared to [^{18}F]-FDOPA, [^{18}F]-FDG, [^{18}F]-fluorodopamine ([^{18}F]-FDA) PET/CT, and CT/MRI, and b) assess the potential eligibility of these patients for treatment with radiolabeled or so-called “cold” SSA.

Patients and Methods

Patients

Between January 2014 and March 2015, 20 consecutive patients (11 men, 9 women) at a mean age of 48.4±14.0 years with histologically confirmed PGLs were prospectively evaluated at the *Eunice Kennedy Shriver* National Institute of Child Health and Human Development (NICHD) of the National Institutes of Health (NIH).

The study protocol was approved by the institutional review board of the *Eunice Kennedy Shriver* NICHD (protocol: 00-CH-0093). All patients provided written informed consent for all clinical, genetic, biochemical, and imaging studies regarding PHEOs/PGLs.

Seven patients had an *SDHD* mutation, 9 patients were positive for *SDHB*, 1 patient was positive for a hypoxia-inducible factor 2 alpha (*HIF2A*) mutation, and 3 patients were apparently sporadic. Sixteen patients presented with additional primary PHEOs/PGLs or metastatic disease (defined as PHEOs/PGLs in sites where chromaffin tissue is normally present) outside of the head and neck region (7 *SDHB*, 7 *SDHD*, 1 *HIF2A*, and 1 apparently sporadic) and/or in the bone. These non-HNPGL lesions were not evaluated in this study. Individual patient characteristics are summarized in Table 2.

Imaging Techniques

CT scans of the neck were performed using the following devices: Siemens Somatom Definition AS, Siemens Somatom Definition Flash, Siemens Medical Solutions; Toshiba Aquilion ONE, Toshiba Medical Systems. Section thickness was up to 3 mm in the neck. All studies were performed with intravenous (i.v.) rapid infusion of 130 milliliter (ml) nonionic water-soluble contrast agent (Isovue 300), at 3-4 ml/second (sec).

MR scans of the neck were obtained with 1.5 and 3 Tesla scanners (Philips Achieva 1.5 and 3 Tesla, Philips Medical Systems; Siemens Verio 1.5 Tesla, Siemens Medical Solutions). Image thickness was 5 millimeter (mm) for all neck studies. Pre- and post-injection images were obtained in the axial plane. All MR scans included axial T2 series with and without fat saturation, STIR series, and T1 pre- and post-contrast series after i.v. injection of a gadolinium-diethylenetriamine pentaacetic acid contrast agent.

All 20 patients underwent [^{68}Ga]-DOTATATE, [^{18}F]-FDOPA, [^{18}F]-FDG PET/CT as well as CT and/or MRI, with 18 also receiving [^{18}F]-FDA PET/CT. Fourteen patients received both a CT and MRI of the neck while 3 patients only received a neck MRI and another 3 patients only underwent a neck CT.

Whole body PET/CT scans from the upper thighs to the skull were performed 60 minutes (min) after i.v. injection with mean doses of 192.4±3.3 Megabecquerel (MBq) [^{68}Ga]-DOTATATE, 30 min after 465.1±7.4 MBq [^{18}F]-FDOPA, 60 min after 314.5±81.4 MBq [^{18}F]-FDG, and approximately 8 min after 38.9±0.8 MBq [^{18}F]-FDA. 60 min before each [^{18}F]-FDOPA scan, 200 milligrams (mg) of carbidopa were administered orally. All PET/CT scans were performed on a Siemens Biograph-mCT 128 PET/CT scanner (Siemens Medical Solutions). PET imaging was obtained in 3D mode. PET images were reconstructed on a 256×256 matrix using an iterative algorithm provided by the manufacturer, which also uses time of flight (TOF). CT studies for attenuation correction and anatomic co-registration were performed without contrast.

Analysis of Data

[^{68}Ga]-DOTATATE PET/CT studies were each read independently by two nuclear medicine physicians blinded to all imaging and clinical data except for the diagnosis, sex, and age of the patients. Maximum standardized uptake values (SUV_{max}) were determined and focal areas of abnormal uptake showing a higher SUV_{max} than surrounding tissue were considered as lesions. In all other imaging studies, physicians were blinded to [^{68}Ga]-DOTATATE PET/CT scans and clinical data except for the diagnosis, sex, and age of the

patients, as well as previous imaging studies. All imaging studies were performed within 3 months of each other.

Histologic proof of all head and neck lesions was not feasible. Therefore, all definite head and neck foci localized with [^{18}F]-FDOPA PET/CT and/or MRI (CT for the 3 patients in whom MRI could not be performed) were presumed to be true positive lesions since these are the imaging modalities of choice for HNPGLs according to the current guidelines (13, 14), with [^{18}F]-FDOPA known to have excellent sensitivity and specificity (2, 10). Since delineation of tympanic and GJ tumors is not always feasible, these lesions were summarized as jugulotympanic (JT) tumors.

Statistics

For statistical analysis, the McNemar test was used to compare sensitivities between [^{68}Ga]-DOTATATE PET/CT and the other imaging modalities. A two-sided $p<0.05$ was considered significant.

Results

Thirty-eight lesions were identified in total on [^{18}F]-FDOPA PET/CT and CT/MRI, with 37 out of 38 lesions (37/38) detected on [^{18}F]-FDOPA PET/CT and 23/38 lesions detected on CT/MRI. All 38 lesions were detected on [^{68}Ga]-DOTATATE PET/CT (mean SUV_{max} 81.1±83.6) as well as 7 additional head and neck lesions ($p=0.016$): 2 JT lesions, 1 GV lesion, 2 CB lesions (all related to patients with *SDHD* mutations), and 2 lymphatic nodes (in a patient with an *SDHB* mutation). Significantly fewer lesions were identified on [^{18}F]-FDG PET/CT (27/38, $p<0.01$) and [^{18}F]-FDA PET/CT (10/34, $p<0.01$). Except for the 7 lesions only detected by [^{68}Ga]-DOTATATE PET/CT, one JT tumor, measuring 1.6 cm on MRI and positive on [^{18}F]-FDG and [^{68}Ga]-DOTATATE PET/CT, was missed on [^{18}F]-FDOPA PET/CT in a patient with an *SDHD* mutation. On CT/MRI, JT lesions and lymphatic nodes, especially, were missed whereas CB and GV tumors were identified relatively reliably. Detailed information about identified lesions and patient characteristics are provided in Tables 1 and 2. Figures 1-3 demonstrate common sites of HNPGLs, lesions only detected by [^{68}Ga]-DOTATATE PET/CT, and patient examples.

Discussion

We present a comparison of [^{68}Ga]-DOTATATE PET/CT to [^{18}F]-FDOPA, [^{18}F]-FDG, [^{18}F]-FDA PET/CT and CT/MRI in a cohort of 20 patients with HNPGLs, 16 with underlying *SDHx*-related mutations, 1 with a *HIF2A* mutation, and 3 apparently sporadic.

On [^{68}Ga]-DOTATATE PET/CT, significantly more lesions were detected compared to any other imaging modality used in this study, thus confirming the utility of [^{68}Ga]-DOTATATE in localizing HNPGLs and determining the possible eligibility of these patients for PRRT.

Functional imaging agents are able to target PHEOs/PGLs through different mechanisms and have shown widely split performances based on the localization and genetics.

[^{18}F]-FDA and [^{123}I]-MIBG specifically target catecholamine synthesis, storage, and secretion pathways. Both enter the cell via the norepinephrine transporter (23, 24), and [^{18}F]-FDA PET/CT had previously shown decent imaging results in the diagnosis and localization of primary and metastatic sympathetic PGLs (25, 26). In this study, only 10 of 34 lesions were detected on [^{18}F]-FDA PET/CT. This confirms previous results in parasympathetic PGLs (10). [^{123}I]-MIBG scintigraphy is known to be inferior to [^{18}F]-FDA PET/CT but might still be useful in identifying patients who could benefit from [^{131}I]-MIBG treatment if they do not qualify for a surgical approach (e.g., multiple HNPGLs, metastatic disease). However, the likelihood of these patients to be positive on [^{123}I]-MIBG is very low.

[^{18}F]-FDG is a sensitive but non-specific radiopharmaceutical and enters the cell via glucose transporters (GLUT) (27). Its accumulation is related to increased glucose metabolism as seen in many different types of tumors (27). *SDHx*-related HNPGLs as well as *SDHx*-related sympathetic PGLs had shown higher glucose uptake compared to sporadic and other hereditary PGLs in previous studies (28, 29) due to an upregulation of hexokinases 2 and 3 (30). Reported detection rates for *SDHx*-related HNPGLs of [^{18}F]-FDG ranged from 77% (10) to 90.5% (29). In our study, 27 out of 38 lesions were detected, resulting in a lower detection rate of 71.1%, although 16 of 20 patients in our study were *SDHx* positive. JT lesions might be missed due to their proximity to the brain, which shows high glucose-uptake as well. Another reason might be that not only the underlying genotype might influence the glucose uptake, but also other mechanisms, which haven't been discovered yet.

[^{18}F]-FDOPA targets cells via the amino acid transporter system (31). It is the currently recommended functional imaging of choice in HNPGLs (13, 14), proven to be very sensitive (greater than CT and MRI) and highly specific (2, 10, 11). This study confirms the strong diagnostic performance of [^{18}F]-FDOPA PET/CT in localizing HNPGLs, identifying significantly more lesions than all other imaging modalities used except [^{68}Ga]-DOTATATE PET/CT (20), which emphazises a possible functional dedifferentiation of the large amino acid transporter in *SDHx* mutations.

Significantly more lesions were identified on [^{68}Ga]-DOTATATE PET/CT compared to all other imaging modalities in this study. No additional lesions were identified on any other imaging modality. PGLs are known to overexpress SSTR (15), and SSTR imaging with [^{111}In]-DTPA-octreotide scintigraphy had already shown strong diagnostic performance in parasympathetic PGLs (32). Since SSTR imaging can be performed using PET/CT and newly developed DOTA-analogs such as DOTATATE, DOTANOC, and DOTATOC bind to SSTR-expressing tumors much more effectively (16), researchers have been focusing on DOTA-peptide imaging in PHEOs/PGLs, including parasympathetic PGLs, and have shown promising results (20, 21, 33-35). Recently, our group demonstrated the superiority of [^{68}Ga]-DOTATATE PET/CT compared to [^{18}F]-FDA, [^{18}F]-FDOPA, [^{18}F]-FDG, and CT/MRI in localizing *SDHB*-related metastatic sympathetic PHEOs/PGLs (22). Our results are in accordance with the increased expression of SSTR2A and SSTR3 found in PHEOs/PGLs with an *SDH* deficiency (36), as the majority of our patients were positive for *SDHx* mutations.

Although false positive findings cannot be fully excluded, the 7 lesions only identified by [^{68}Ga]-DOTATATE PET/CT most likely belong to PGL manifestations for several reasons: five of these lesions were found in typical locations for HNPGLs, all patients had confirmed PGLs, and all of these lesions were seen in patients with *SDHx* mutation-related disease, who are at high risk for multiple primary or metastatic lesions.

Besides its diagnostic value, [^{68}Ga]-DOTATATE PET/CT is used to determine which patients may benefit from PRRT since surgery is not always feasible for those with multiple or metastatic lesions. PRRT is an established treatment option in gastroenteropancreatic NETs (37) and its successful use has already been reported in a limited number of patients with HNPGLs (17, 19). However, PRRT has not been specifically evaluated in a larger series of patients with HNPGLs or in *SDHx*-related PHEOs/PGLs yet. Additionally, it is currently not approved by the United States Food and Drug Administration.

The high detection rate of HNPGLs on [^{68}Ga]-DOTATATE PET/CT, confirming their SSTR2 expression, may also suggest that these patients can be treated with so-called “cold” SSTR analogs, including sandostatin LAR, lanreotide, or others. Although this has not yet been evaluated in HNPGLs, data from studies using lanreotide in gastroenteropancreatic NETs (38) and individual reports of octreotide treatment in patients with HNPGLs support this approach (18, 39).

Anatomical imaging using CT/MRI is a main component of the diagnostic work-up of HNPGLs, with their greatest strength being the ability to estimate tumor delineation. However, functional imaging with [^{18}F]-FDOPA and [^{68}Ga]-DOTATATE PET/CT provides a higher sensitivity (10, 11, 21), and the advantage of whole body imaging, which is especially important in the evaluation of patients with hereditary disease because of their increased risk for multiplicity and metastases. In our study lesions were missed by CT/MRI especially in the JT region. This might have been avoidable by performing 3D-TOF or 4D-MR angiographic sequences, which seem to be more sensitive in detecting HNPGLs (2).

Limitations in our study consist of its small number of patients, with a significant portion having *SDHB* mutations (although *SDHD* mutations are more common in HNPGLs), a disproportionally low number of patients with apparently sporadic tumors, the lack of patients with underlying *SDHC* mutations, and a disproportionally high number of patients with metastatic disease. Furthermore, as already mentioned, histological proof was not feasible for the majority of lesions, including those that were only positive on [^{68}Ga]-DOTATATE PET/CT.

Conclusion

[^{68}Ga]-DOTATATE PET/CT demonstrated excellent diagnostic value in the localization of *SDHx*-related and sporadic HNPGLs, also confirming the possible eligibility of these patients for treatment with radiolabeled or “cold” SSA. Significantly more lesions were identified on [^{68}Ga]-DOTATATE PET/CT compared to all other functional and anatomical imaging modalities, including [^{18}F]-FDOPA PET/CT—the current gold standard of functional imaging for these tumors. Due to these results and the increasing availability and

use of DOTA-analogs in the therapy of neuroendocrine tumors, we expect that [^{68}Ga]-DOTATATE PET/CT will become the preferred functional imaging modality for HNPGLs in the near future.

Acknowledgments

Financial support: This work was supported, in part, by the Intramural Research Program of the National Institutes of Health, *Eunice Kennedy Shriver* National Institute of Child Health and Human Development.

References

1. Martin TP, Irving RM, Maher ER. The genetics of paragangliomas: a review. Clin Otolaryngol. 2007; 32:7–11. [PubMed: 17298303]
2. Taieb D, Kaliski A, Boedeker CC, et al. Current approaches and recent developments in the management of head and neck paragangliomas. Endocr Rev. 2014; 35:795–819. [PubMed: 25033281]
3. Sykes JM, Ossoff RH. Paragangliomas of the head and neck. Otolaryngol Clin North Am. 1986; 19:755–767. [PubMed: 3797012]
4. Piccini V, Rapizzi E, Bacca A, et al. Head and neck paragangliomas: genetic spectrum and clinical variability in 79 consecutive patients. Endocr Relat Cancer. 2012; 19:149–155. [PubMed: 22241717]
5. Baysal BE, Willett-Brozick JE, Lawrence EC, et al. Prevalence of SDHB, SDHC, and SDHD germline mutations in clinic patients with head and neck paragangliomas. J Med Genet. 2002; 39:178–183. [PubMed: 11897817]
6. Neumann HP, Erlic Z, Boedeker CC, et al. Clinical predictors for germline mutations in head and neck paraganglioma patients: cost reduction strategy in genetic diagnostic process as fall-out. Cancer Res. 2009; 69:3650–3656. [PubMed: 19351833]
7. Erickson D, Kudva YC, Ebersold MJ, et al. Benign paragangliomas: clinical presentation and treatment outcomes in 236 patients. J Clin Endocrinol Metab. 2001; 86:5210–5216. [PubMed: 11701678]
8. Neumann HP, Pawlu C, Peczkowska M, et al. Distinct clinical features of paraganglioma syndromes associated with SDHB and SDHD gene mutations. JAMA. 2004; 292:943–951. [PubMed: 15328326]
9. Pacak K, Eisenhofer G, Goldstein DS. Functional imaging of endocrine tumors: role of positron emission tomography. Endocr Rev. 2004; 25:568–580. [PubMed: 15294882]
10. King KS, Chen CC, Alexopoulos DK, et al. Functional imaging of SDHx-related head and neck paragangliomas: comparison of 18F-fluorodihydroxyphenylalanine, 18F-fluorodopamine, 18F-fluoro-2-deoxy-D-glucose PET, 123I-metaiodobenzylguanidine scintigraphy, and 111In-pentetreotide scintigraphy. J Clin Endocrinol Metab. 2011; 96:2779–2785. [PubMed: 21752889]
11. Hoegerle S, Ghanem N, Altehoefer C, et al. F-18-DOPA positron emission tomography for the detection of glomus tumours. European Journal of Nuclear Medicine and Molecular Imaging. 2003; 30:689–694. [PubMed: 12618904]
12. Treglia G, Cocciolillo F, de Waure C, et al. Diagnostic performance of 18F-dihydroxyphenylalanine positron emission tomography in patients with paraganglioma: a meta-analysis. Eur J Nucl Med Mol Imaging. 2012; 39:1144–1153. [PubMed: 22358431]
13. Lenders JW, Duh QY, Eisenhofer G, et al. Pheochromocytoma and paraganglioma: an endocrine society clinical practice guideline. J Clin Endocrinol Metab. 2014; 99:1915–1942. [PubMed: 24893135]
14. Taieb D, Timmers HJ, Hindie E, et al. EANM 2012 guidelines for radionuclide imaging of phaeochromocytoma and paraganglioma. Eur J Nucl Med Mol Imaging. 2012; 39:1977–1995. [PubMed: 22926712]

15. Reubi JC, Waser B, Schaer JC, Laissue JA. Somatostatin receptor sst1-sst5 expression in normal and neoplastic human tissues using receptor autoradiography with subtype-selective ligands. Eur J Nucl Med. 2001; 28:836–846. [PubMed: 11504080]
16. Reubi JC, Schar JC, Waser B, et al. Affinity profiles for human somatostatin receptor subtypes SST1-SST5 of somatostatin radiotracers selected for scintigraphic and radiotherapeutic use. Eur J Nucl Med. 2000; 27:273–282. [PubMed: 10774879]
17. Zovato S, Kumanova A, Dematte S, et al. Peptide receptor radionuclide therapy (PRRT) with 177Lu-DOTATATE in individuals with neck or mediastinal paraganglioma (PGL). Horm Metab Res. 2012; 44:411–414. [PubMed: 22566197]
18. Elshafie O, Al Badaai Y, Alwahaibi K, et al. Catecholamine-secreting carotid body paraganglioma: successful preoperative control of hypertension and clinical symptoms using high-dose long-acting octreotide. Endocrinol Diabetes Metab Case Rep. 2014; 2014:140051. [PubMed: 25136449]
19. Puranik AD, Kulkarni HR, Singh A, Baum RP. Peptide receptor radionuclide therapy with Y/Lu-labelled peptides for inoperable head and neck paragangliomas (glomus tumours). Eur J Nucl Med Mol Imaging. 2015
20. Kroiss A, Putzer D, Frech A, et al. A retrospective comparison between 68Ga-DOTA-TOC PET/CT and 18F-DOPA PET/CT in patients with extra-adrenal paraganglioma. Eur J Nucl Med Mol Imaging. 2013; 40:1800–1808. [PubMed: 24072345]
21. Sharma P, Thakar A, Suman KCS, et al. 68Ga-DOTANOC PET/CT for baseline evaluation of patients with head and neck paraganglioma. J Nucl Med. 2013; 54:841–847. [PubMed: 23520216]
22. Janssen I, Blanchet EM, Adams K, et al. Superiority of [68Ga]-DOTATATE PET/CT to other functional imaging modalities in the localization of SDHB-associated metastatic pheochromocytoma and paraganglioma. Clin Cancer Res. 2015
23. Sisson JC, Wieland DM. Radiolabeled meta-iodobenzylguanidine: pharmacology and clinical studies. Am J Physiol Imaging. 1986; 1:96–103. [PubMed: 3330445]
24. Timmers HJ, Eisenhofer G, Carrasquillo JA, et al. Use of 6-[18F]-fluorodopamine positron emission tomography (PET) as first-line investigation for the diagnosis and localization of non-metastatic and metastatic phaeochromocytoma (PHEO). Clin Endocrinol (Oxf). 2009; 71:11–17. [PubMed: 19138315]
25. Timmers HJ, Chen CC, Carrasquillo JA, et al. Comparison of 18F-fluoro-L-DOPA, 18F-fluoro-deoxyglucose, and 18F-fluorodopamine PET and 123I-MIBG scintigraphy in the localization of pheochromocytoma and paraganglioma. J Clin Endocrinol Metab. 2009; 94:4757–4767. [PubMed: 19864450]
26. Ilias I, Chen CC, Carrasquillo JA, et al. Comparison of 6-18F-fluorodopamine PET with 123I-metaiodobenzylguanidine and 111in-pentetreotide scintigraphy in localization of nonmetastatic and metastatic pheochromocytoma. J Nucl Med. 2008; 49:1613–1619. [PubMed: 18794260]
27. Belhocine T, Spaepen K, Dusart M, et al. 18FDG PET in oncology: the best and the worst (Review). Int J Oncol. 2006; 28:1249–1261. [PubMed: 16596242]
28. Timmers HJ, Chen CC, Carrasquillo JA, et al. Staging and functional characterization of pheochromocytoma and paraganglioma by 18F-fluorodeoxyglucose (18F-FDG) positron emission tomography. J Natl Cancer Inst. 2012; 104:700–708. [PubMed: 22517990]
29. Blanchet EM, Gabriel S, Martucci V, et al. 18F-FDG PET/CT as a predictor of hereditary head and neck paragangliomas. Eur J Clin Invest. 2014; 44:325–332. [PubMed: 24422786]
30. van Berkel A, Rao JU, Kusters B, et al. Correlation Between In Vivo 18F-FDG PET and Immunohistochemical Markers of Glucose Uptake and Metabolism in Pheochromocytoma and Paraganglioma. J Nucl Med. 2014
31. Havekes B, King K, Lai EW, Romijn JA, Corssmit EP, Pacak K. New imaging approaches to phaeochromocytomas and paragangliomas. Clin Endocrinol (Oxf). 2010; 72:137–145. [PubMed: 19508681]
32. Koopmans KP, Jager PL, Kema IP, Kerstens MN, Albers F, Dullaart RP. 111In-octreotide is superior to 123I-metaiodobenzylguanidine for scintigraphic detection of head and neck paragangliomas. J Nucl Med. 2008; 49:1232–1237. [PubMed: 18632829]

33. Maurice JB, Troke R, Win Z, et al. A comparison of the performance of (6)(8)Ga-DOTATATE PET/CT and (1)(2)(3)I-MIBG SPECT in the diagnosis and follow-up of phaeochromocytoma and paraganglioma. Eur J Nucl Med Mol Imaging. 2012; 39:1266–1270. [PubMed: 22526961]

34. Naji M. AAL-N. (6)(8)Ga-labelled peptides in the management of neuroectodermal tumours. Eur J Nucl Med Mol Imaging. 2012; 39(Suppl 1):S61–67. [PubMed: 22388623]

35. Naji M, Zhao C, Welsh SJ, et al. 68Ga-DOTA-TATE PET vs. 123I-MIBG in identifying malignant neural crest tumours. Mol Imaging Biol. 2011; 13:769–775. [PubMed: 20700766]

36. Elston MS, Meyer-Rochow GY, Conaglen HM, et al. Increased SSTR2A and SSTR3 expression in succinate dehydrogenase-deficient pheochromocytomas and paragangliomas. Hum Pathol. 2014

37. Kwekkeboom DJ, de Herder WW, Kam BL, et al. Treatment with the radiolabeled somatostatin analog [177 Lu-DOTA 0,Tyr3]octreotate: toxicity, efficacy, and survival. J Clin Oncol. 2008; 26:2124–2130. [PubMed: 18445841]

38. Caplin ME, Pavel M, Cwikla JB, et al. Lanreotide in metastatic enteropancreatic neuroendocrine tumors. N Engl J Med. 2014; 371:224–233. [PubMed: 25014687]

39. Kau R, Arnold W. Somatostatin receptor scintigraphy and therapy of neuroendocrine (APUD) tumors of the head and neck. Acta Otolaryngol. 1996; 116:345–349. [PubMed: 8725546]

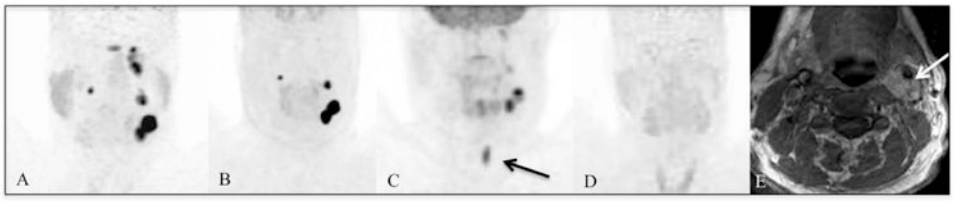

Figure 1.

Patient 5 with *SDHD* mutation-related HNPGLs. [^{68}Ga]-DOTATATE PET/CT (A) demonstrates a lobulated finding in the CB region on the left side, additional lesions in the GV region on both sides, and in the JT region on the left side. The findings in the JT region are not visible on [^{18}F]-FDOPA PET/CT (B). [^{18}F]-FDG PET/CT (C) demonstrates the left CB and very faintly the GV and part of the JT lesions on the left side. The black arrow points to uptake in the vocal cord. [^{18}F]-FDA PET/CT (D) is completely negative. The white arrow on the MRI (E) points to the CB lesion on the left side.

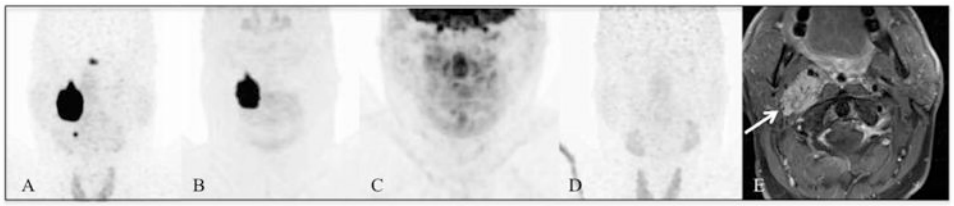

Figure 2.

Patient 18 with *SDHD* mutation-related HNPGLs. [^{68}Ga]-DOTATATE PET/CT (A) demonstrates a big mass in the GV region on the right side and an additional lesion in the CB region on the right. The finding in the CB region is not visible on [^{18}F]-FDOPA PET/CT (B). The [^{18}F]-FDG PET/CT (C) and [^{18}F]-FDA PET/CT (D) scans are completely negative. The arrow on the MRI (E) points to the GV lesion on the right side.

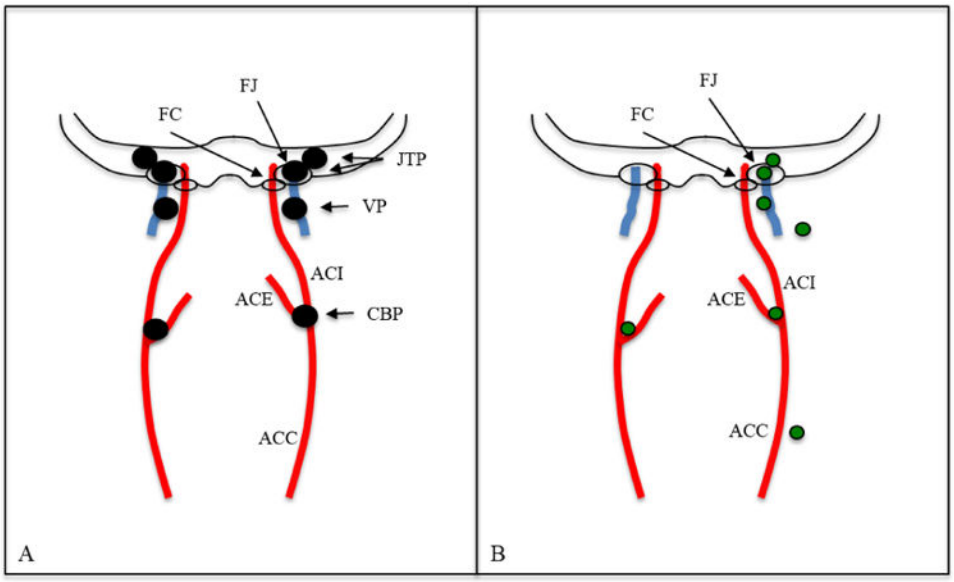

Figure 3.

(A) Common sites of HNPGLs (black). (B) Localization of lesions detected only on [^{68}Ga]-DOTATATE in our study (green). Abbreviations: ACC: common carotid artery, ACE: external carotid artery, ACI: internal carotid artery; CBP: carotid body paraganglioma, FC: carotid foramen, FJ: jugular foramen, JTP: jugulotympanic paraganglioma, VP: vagale paraganglioma.

Table 1

Identified head and neck lesions on [^{68}Ga]-DOTATATE-, [^{18}F]-FDA-, [^{18}F]-FDOPA-, [^{18}F]-FDG-PET/CT, and CT/MRI compared to lesions identified by the imaging comparator.

	[^{68}Ga] -DOTATATE	[^{18}F]-FDOPA	[^{18}F]-FDG	[^{18}F]-FDA	CT/MRI
JT	12/12	11/12	8/12	4/10	5/12
CB	10/10	10/10	9/10	0/10	8/10
GV	8/8	8/8	6/8	3/7	7/8
LN	8/8	8/8	4/8	3/7	3/8
Total	38/38	37/38	27/38	10/34	23/38

Abbreviations: JT, jugulotympanic; CB, carotid body, GV, glomus vagale; LN, lymphatic node

Table 2

Individual patient and lesion characteristics.

Patient	Sex	Mutation	AAD	Metastatic or other primary	Hypersecretion	Lesion	Size on CT/MRI	[^{68}Ga]-DOTATATE	[^{18}F]-FDOPA	[^{18}F]-FDG	[^{18}F]-FDA
1	m	*SDHB*	21	yes	none	R JT	1,8 cm	+	+	+	+
						R LN Level II	0,5 cm*	+	-	-	-
						R LN Level III	0,6 cm*	+	+	-	-
						R LN Level III	0,5 cm*	+	+	-	-
						R LN Level IV	0,4 cm*	+	-	-	-
2	f	*SDHB*	22	yes	none	L CB	nv	+	+	+	-
3	m	*SDHB*	52	yes	NMN, NE, MTT, DA	R JT	2,8 cm	+	+	+	+
4	f	as	65	no	None	R JT	2,4 cm	+	+	-	+
5	m	*SDHD*	19	yes	NMN,NE,CgA	L JT	nv	+	-	-	-
						L JT	nv	+	-	-	-
						L JT	1,6 cm	+	-	+	-
						L GV	1,0 cm	+	+	+	-
						L CB	2,4 cm	+	+	+	-
						R GV	nv	+	+	-	-
6	f	*HIF2A*	34	yes	none	L JT	nv	+	+	-	+
7	m	*SDHD*	62	yes	NMN, NE, CgA	L GV	1,2 cm	+	+	+	np
8	f	*SDHB*	19	yes	NMN	R JT	0,7 cm	+	+	+	np
						R JT	1,0 cm	+	+	+	np
						R LN Level II	0,7 cm*	+	+	+	np
9	f	*SDHB*	37	no	DA, MTT	R CB	2,9 cm	+	+	+	-
10	m	*SDHB*	36	yes	NMN	R CB	1,4 cm	+	+	+	-
11	f	*SDHD*	43	yes	none	R JT	Nv	+	+	-	-

Patient	Sex	Mutation	AAD	Metastatic or other primary	Hypersecretion	Lesion	Size on CT/MRI	[^{68}Ga]-DOTATATE	[^{18}F]-FDOPA	[^{18}F]-FDG	[^{18}F]-FDA
						L JT	Nv	+	+	-	-
						R GV	Nv	+	+	-	-
						R LN level II	Nv	+	+	-	-
						R CB	5,0 cm	+	+	+	-
						L CB	4,7 cm	+	+	+	-
12	m	*SDHB*	35	no	none	R JT	Nv	+	+	+	-
						L JT	Nv	+	+	+	-
						L CB	5,0 cm	+	+	+	-
13	m	as	55	no	MTT	R GV	4,3 cm	+	+	+	+
14	m	*SDHB*	47	yes	DA, MTT	L CB	1,8 cm	+	+	+	-
15	f	*SDHB*	47	yes	DA, MTT, CgA	L CB	Nv	+	+	-	-
16	f	*SDHD*	13	yes	MTT	L GV	Nv	+	-	-	-
						L CB	Nv	+	-	-	-
17	m	as	39	yes	NMN, DA, MTT, CgA	R GV	5,7 cm	+	+	+	+
18	f	SDHD	28	yes	DA, MTT, CgA	R GV	2,8 cm	+	+	+	+
						R LN level IV	0,7 cm*	+	+	+	+
						R LN level III	1,5 cm	+	+	+	+
						L LN level IV	3,5 cm	+	+	+	+
19	m	SDHD	43	yes	none	R GV	3,5 cm	+	+	+	-
						R CB	Nv	+	-	-	-
20	m	SDHD	23	N yes	none	R JT	Nv	+	+	-	-
						R CB	2,2 cm	+	+	+	-
						L LN level IV	Nv	+	+	-	-

Abbreviations: AAD, age at diagnosis; as, apparently sporadic; CB, carotid body; CgA, chromogranin A; cm, centimeter; DA, dopamine; f, female, GV, glomus vagale; JT, jugulotympanic; L, left side; LN, lymphatic node; m, male; MTT, methoxytyramine, NE, norepinephrine; NMN, normetanephrine; np, not performed; nv, not visible; R, right side; +, positive; -, negative;

*considered as normal LN on CT/MRI.